Journal of Applied Polymer Science

Functionalized *N*-(4-Hydroxy phenyl) Maleimide Monomers: Kinetics of Thermal Polymerization and Degradation Using Model-Free Approach

G. Pitchaimari, C. T. Vijayakumar
Department of Polymer Technology, Kamaraj College of Engineering and Technology, K. Vellakulam (Post) 625 701 TamilNadu, India
Correspondence to: C. T. Vijayakumar (E-mail: ctvijay22@yahoo.com)

ABSTRACT: *N*-(4-Hydroxy phenyl) maleimide (HPMI) is prepared and is functionalized with acryloyl, methacryloyl, allyl, propargyl, and cyanate groups. The structural and thermal characterizations of the materials are done using FTIR, NMR, DSC, and TGA. Curing and degradation kinetics are performed using Flynn–Wall–Ozawa, Vyazovkin, and Friedman methods. Activation energies (E_a) for the polymerization of the synthesized monomers varied and are dependent on the nature of the functional group present in HPMI. The propargyl functionalized monomer shows the highest E_a values whereas the methacryloyl functionalized monomer shows the lowest E_a values. In the case of thermal degradation of the polymerized materials, the apparent E_a values for acryloyl, methacryloyl and cyanate functionalized materials are slightly higher than that of poly-HPMI (PHPMI). The thermally cured allyl and propargyl functionalized materials show a different trend and may be attributed to the complications arising due to Claisen rearrangement reaction during the thermal curing. © 2013 Wiley Periodicals, Inc. J. Appl. Polym. Sci. **2014**, *131*, 39935.

KEYWORDS: polyimides; thermal properties; thermogravimetric analysis (TGA)

Received 15 May 2013; accepted 5 September 2013
DOI: 10.1002/app.39935

INTRODUCTION

Thermally stable polymers are placed under the category high performance polymers because of their wide range of applications in demanding environments. Heat resistance or thermally stable polymers are used as electric insulators, enamels, protective coating, etc.[1–3] Polymaleimides and copolymaleimides belong to thermally stable polymers. The polymers of N-substituted maleimides usually have high heat resistance but they cannot be used as engineering plastics because of the difficulty in processing due to their high glass transition temperatures.[4]

Maleimide monomers are having rigid molecular structures and the five-membered planar rings present in the chain hinder the rotation of the imide group around the backbone chain of the macromolecules.[5,6] These lead to high melting temperature and poor solubility in common organic solvents. Further the cured maleimide resins have high cross linking density and rigid molecular networks, which result in an inherent brittleness. Most thermosets incorporate particulate fillers or fiber reinforcement to reduce cost, to modify physical properties, to reduce shrinkage during cure and to improve flame retardance.

The synthesis of monomers containing different active functional groups is of special interest.[7–9] Many studies have been carried out on synthesis, thermal stability and solid state decomposition kinetics of methacrylate polymers containing various ester moieties as well as on preparing porous polymer structures by using different acrylates and methacrylates.[10,11] The high performance thermosets like allyl and propargyl terminated resins[12] were being developed for the fabrication of composite materials which can have continuous service at high temperatures.

Polycyanurates derived from the thermal cure of aromatic dicyanate esters possess many attractive physical, dielectric and mechanical properties. However, the thermal characteristics are inferior to those of conventional bismaleimide systems. Blends of aromatic dicyanate esters and bismaleimide have been realized to derive systems bearing good physicochemical attributes of the two components, i.e., the thermal characteristics of bismaleimide and the toughness of polycyanurates.

Taking into consideration the thermal stability of the polymerized bismaleimide compounds, it is intended to develop maleimide unit bearing monomers which are curable by UV and e beam radiations. In the previous investigations, *N*-(4-hydroxy phenyl) maleimide (HPMI) is functionalized with different crosslinkable groups (acryloyl, methacryloyl, allyl, propargyl, cyanate and epoxy). The structures of the synthesized materials were characterized by FTIR, ^{1}H-NMR, and ^{13}C-NMR. The nature of the thermal curing of these functionalized maleimide monomers were investigated using DSC. The thermal curing was carried out at the appropriate temperature in an oxygen-

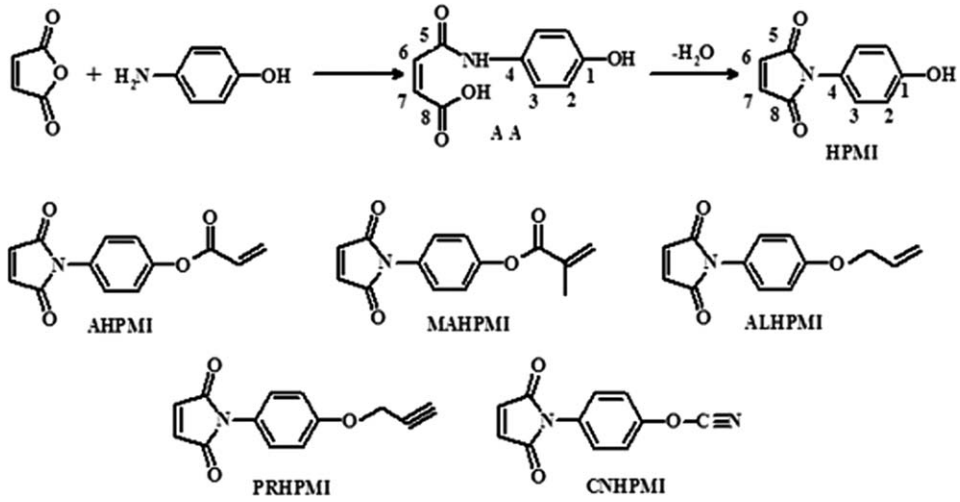

Scheme 1. Preparation of *N*-(4-hydroxy phenyl) maleimide (HPMI) and the structures of synthesized monomers (AHPMI, MAHPMI, ALHPMI, PRHPMI, and CNHPMI).

free dry nitrogen atmosphere. The thermal stabilities of these materials were also investigated using TGA.

Model fitting kinetic methods are used to determine the kinetic triplets using multiple heating rate programs and the kinetic triplet obtained from these methods for nonisothermal condition is highly uncertain and cannot be compared with the kinetic triplets obtained from isothermal condition.[13,14] Vyazovkin (VYZ) model-free approach through use of isoconversion method leads to a trust worthy way of obtaining reliable and consistent kinetic information from nonisothermal data from DSC and TG studies. The variation of the activation energy with the extent of conversion helps to reveal the complexity of multiple reactions taking place during thermal degradation of materials.[15–18] Hence in the present study the apparent activation energy for the polymerization of the functionalized monomers and thermal degradation of the polymers are obtained using three model-free kinetic [Flynn–Wall–Ozawa (FWO), Vyazovkin (VYZ), and Friedman (FRD)] methods. The results obtained are compared. This study has been carried out to understand the curing behavior, to establish the curing schedule and to know the energetics of the degradation process.

EXPERIMENTAL

Materials

Maleic anhydride was purchased from Central Drug House (P), New Delhi 110 002. 4-Amino phenol, *p*-toluene sulfonic acid, allyl chloride, and cyanogen bromide were purchased from Loba Chemie, Mumbai 400 002. Hydroquinone was obtained from Qualigens Fine Chemicals, Mumbai 400 025. Acrylic acid, acetone, benzoyl chloride, *N,N′*-dimethyl formamide, methacrylic acid, tetrabutyl ammonium chloride, tetrahydrofuran, triethylamine, and toluene were purchased from MERCK Specialist, Mumbai 400 018. Propargyl chloride was obtained from Grauer & Weil (India), Vapi 369 195. All the chemicals were used as received.

Synthesis of Amic Acid

Exactly 53.5 g of 4-amino phenol was dissolved in 500 mL of acetone with constant stirring at room temperature. To this solution, 47 g of powdered maleic anhydride was added in portions. Yellow precipitate was formed and stirred continuously for half an hour. The slurry was filtered and washed with ice cold acetone to remove the acetone soluble materials and dried. The yield was 98% (Scheme 1). FTIR (KBr disc): 3105 cm^{-1} (—OH), 3284 cm^{-1} (—NH), 1712 cm^{-1} (C═O), 1601 cm^{-1} (aromatic ring) and 838 cm^{-1} (HC═CH); ^{1}H-NMR (DMSO-d_6): 6.78 (C_2—H), 7.48 (C_3—H), 6.90 (C_6—H), 6.38 (C_6—H), 4.1 (phenolic —OH), 7.54 (—NH), 8.86 (carboxylic —OH). ^{13}C-NMR (100 MHz, DMSO-d_6): 150.08 (C_1), 113.34 (C_2), 123.56 (C_3), 132.41 (C_4), 161.24 (C_5), 138.18 (C_6), 132.35 (C_7), 169.76 (C_8) ppm.

Synthesis of *N*-(4-Hydroxy phenyl) Maleimide

The yellow amic acid 17.1 g (0.08 mol) was dispersed in a 250 mL round bottom flask containing 73 mL of toluene. *p*-toluene sulfonic acid (1.12 g) and *N,N′*-dimethyl formamide (8 mL) were added into the reaction mixture and refluxed for 3 h. The brown color solution was poured into large quantities of crushed ice and *N*-(4-hydroxy phenyl) maleimide was obtained as yellow precipitate. The material was filtered, washed with ice cold water and dried in vacuum. The molecular formula of the material is $C_{10}H_7NO_3$. The yield was 70% and the material melts at 185°C (Scheme 1). FTIR (KBr disc): 3481 cm^{-1} (—OH), 3101 cm^{-1} (aromatic —CH), 1712 cm^{-1} (C═O), 1601 cm^{-1} (aromatic ring) and 1604 cm^{-1} (HC═CH of maleimide); ^{1}H-NMR (300 MHz, DMSO-d_6, ppm): 6.78 (C_2—H), 7.48 (C_3—H), 6.90 (C_6—H), 3.5 (phenolic —OH) ppm. ^{13}C-NMR (100 MHz, DMSO-d_6, ppm): 157.06 (C_1), 115.45 (C_2), 122.54 (C_3), 134.55 (C_4), 157.54 (C_5), 134.58 (C_6) ppm.

Experimental procedure for the synthesis and characterization of *N*-(4-acryloyloxy phenyl) maleimide (AHPMI), *N*-(4-methacryloyloxy phenyl) maleimide (MAHPMI), *N*-(4-allyloxy phenyl) maleimide (ALHPMI), *N*-(4-propargyloxy phenyl) maleimide (PRHPMI), and *N*-(4-cyanato phenyl) maleimide (CNHPMI) is already presented in the previous work.[19] The structures of all the monomers involved in the present work are presented in Scheme 1.

Thermal Curing

The HPMI and the functionalized monomers were taken in a separate micro test tubes and flushed with dry oxygen-free nitrogen and thermally polymerized (HPMI = 273°C, AHPMI = 247°C, MAHPMI = 214°C, ALHPMI = 180°C, PRHPMI = 240°C, and CNHPMI = 230°C) for 3 h. After the polymerization, the samples were removed from the micro test tubes, ground to coarse powder, packed and stored for further analysis.

Swelling Experiment

The swelling behavior of PHPMI, PAHPMI, PMAHPMI, PPRHPMI, and PCNHPMI were carried out in toluene at 27°C. The weights were measured made using an electronic balance (Shimadzu AUX120, Japan) having an accuracy of 0.1 mg. Pre weighed synthesized polymers were immersed in toulene. After specific intervals of the time (4 h), the polymers were removed from the medium, the surface adhered liquid drops were wiped with blotting paper and the increase in weight was measured. The measurements were continued till the weights of the swollen polymers attained constant values. The swelling ratio (SR %) was calculated,[20] using the following expression.

$$\mathrm{SR}(\%)=\frac{\text{Weight of the swollen polymer -Weight of the dry polymer}}{\text{Weight of the dry polymer}}\times 100 \tag{1}$$

Methods

The FTIR spectra of the materials were recorded using Fourier-transform infrared spectrophotometer-8400S, Shimadzu, Japan by employing KBr disc technique. The differential scanning calorimetric (DSC) curves for *N*-(4-hydroxy phenyl) maleimide (HPMI) and its functionalized materials AHPMI, MAHPMI, ALHPMI, PRHPMI, and CNHPMI were recorded in a TA Instruments DSC Q20. Nearly 2–4 mg of the materials were taken in Tzero aluminum pan and heated from ambient to 400°C by different heating rates (10, 20, and 30°C min^{-1}). Dry nitrogen gas was used to provide the inert atmosphere. The thermogravimetric (TG) curve for all the thermally cured materials poly-HPMI (PHPMI), poly-AHPMI (PAHPMI), poly-MAHPMI (PMAHPMI), poly-ALHPMI (PALHPMI), poly-PRHPMI (PPRHPMI), and poly-CNHPMI (PCNHPMI) were recorded in TA Instruments TGA Q50. The samples (nearly 4–5 mg) were taken in platinum pan and heated from ambient to 800°C at different heating rates (10, 20, and 30°C min^{-1}) in nitrogen atmosphere (balance purge = 40 mL min^{-1} and sample purge = 60 mL min^{-1}).

Kinetic Analysis

If the curing process occurs only by the thermal method, the reaction rate ($d\alpha/dT$) can be obtained by division of the peak height (dH/dT) at temperature T by the total enthalpy of the curing reaction,[21] that is

$$da/dT=(dH/dT)/\Delta H_c \tag{2}$$

where ΔH_c is the total enthalpy of curing. The fractional conversion (α) can be obtained by the measurement of the partial area of the curing peak:

$$\alpha=\Delta H_T/\Delta H_c \tag{3}$$

where ΔH_T is the enthalpy of the area of the curing peak at a particular temperature.

The reaction extent (α) for the degradation reaction is shown in the following equation

$$\alpha=\left(\frac{W_\circ-W_T}{W_\circ-W_e}\right) \tag{4}$$

where W_o is the weight at initial, W_T is the weight at the particular temperature, and W_e is the weight at the end of the degradation process.

The rate of solid-state reactions can be described as

$$\frac{d\alpha}{dt}=k(T)f(\alpha) \tag{5}$$

where $d\alpha/dt$ is the rate of the reaction, $k(T)$ is the rate constant, $f(\alpha)$ is the reaction model. According to Arrhenius's equation, the temperature-dependent rate constant, $k(T)$ is defined as

$$k(T)=A\exp\left(-\frac{E_a}{RT}\right) \tag{6}$$

where A is the pre-exponential factor, E_a is the apparent activation energy, R is the gas constant and T is the tempera
ture.

Flynn–Wall–Ozawa Method

The FWO method is widely used for dynamic kinetic analysis and does not require any assumptions to be made about the conversion dependence.[22] The equation used for this method is given as follows:

$$E_a=\frac{-R}{1.052}\frac{\Delta\ln\beta}{\Delta(1/T)} \tag{7}$$

where E_a is apparent activation energy, R is the gas constant, β is the heating rate, and T is the temperature. In this method, plots of ln β versus $1/T$ give parallel lines for each α value. The slope of these lines gives apparent activation energy, as per the expression.

$$\text{Slope}=-0.4567(E_a/R) \tag{8}$$

Vyazovkin Method

The integration form of Arrhenius equation is given below

$$g(\alpha)=\int_0^\alpha\frac{d\alpha}{f(\alpha)}=A\int_0^t\exp\left(\frac{-E_a(\alpha)}{RT}\right)dt=AJ[E_a(a),T] \tag{9}$$

where $g(\alpha)$ is the integral form of the reaction model $f(\alpha)$ and $T(t)$ is the heating program and A is the Arrhenius constant.

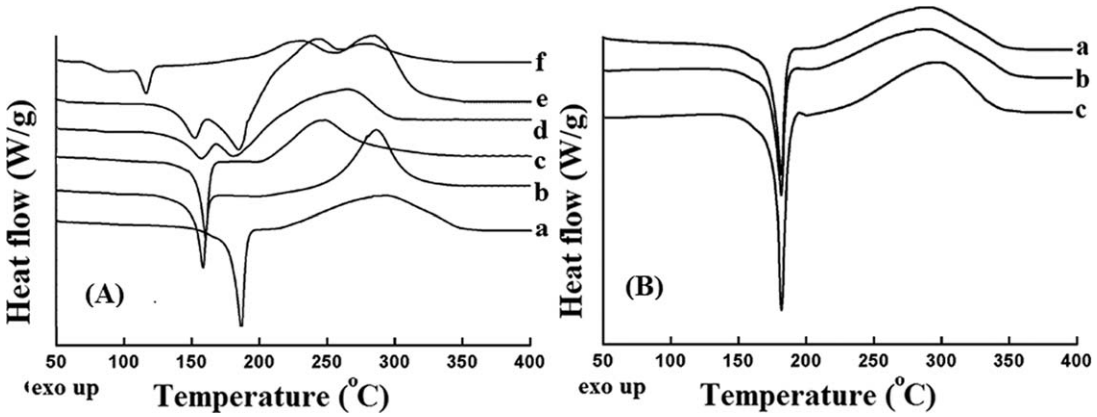

Figure 1. DSC traces of HPMI and its functionalized monomers at a heating rate of 20°C/min (A): (a) HPMI, (b) AHPMI, (c) MAHPMI, (d) ALHPMI, (e) PRHPMI, and (f) CNHPMI. DSC traces of HPMI at different β's (B): (a) 10, (b) 20, and (c) 30. The curves are shifted in the y axis uniformly for clarity.

With a linear heating rate of $\beta = dT/dt$, $T(t)$ is linear and in eq. (9), dt can be substituted by dT/β.

$$g(\alpha)=\int_0^{\alpha}\frac{d\alpha}{f(\alpha)}=\frac{A}{\beta}\int_0^{t}\exp\left(\frac{-E_a(\alpha)}{RT}\right)dT=\frac{AI}{\beta}[E_a(\alpha),T] \qquad (10)$$

Many authors made the numerical approximations to solve the temperature integrals (I and J) and the results of model-free kinetic analysis differ widely depending on the choice of numerical approximations.[23–26] To avoid this dependence on the numerical approximation, Vyazovkin and Dollimore used the fact that for any heating rate β, $g(\alpha)$ is constant. Thus, with heating rates β_1, β_2, and β_3 three integrals are obtained $[g(\alpha)_{\beta 1} = g(\alpha)_{\beta 2} = g(\alpha)_{\beta 3}]$.

$$\frac{A}{\beta_1}I[E_a(\alpha),T]_1=\frac{A}{\beta_2}I[E_a(\alpha),T]_2=\frac{A}{\beta_3}I[E_a(\alpha),T]_3 \qquad (11)$$

Consequently, A can be truncated and six equations can be formulated.[27]

$$\frac{I[E_a(\alpha),T]_1\beta_2}{I[E_a(\alpha),T]_2\beta_1}=1 \qquad (12)$$

$$\frac{I[E_a(\alpha),T]_1\beta_2}{I[E_a(\alpha),T]_2\beta_2}=1 \qquad (13)$$

$$\frac{I[E_a(\alpha),T]_1\beta_3}{I[E_a(\alpha),T]_3\beta_1}=1 \qquad (14)$$

$$\frac{I[E_a(\alpha),T]_3\beta_1}{I[E_a(\alpha),T]_1\beta_3}=1 \qquad (15)$$

$$\frac{I[E_a(\alpha),T]_2\beta_3}{I[E_a(\alpha),T]_3\beta_2}=1 \qquad (16)$$

$$\frac{I[E_a(\alpha),T]_3\beta_2}{I[E_a(\alpha),T]_2\beta_3}=1 \qquad (17)$$

The summarized equation for the above is given below.

$$\sum_{i=1}^{n}\sum_{j\neq 1}^{n}\frac{I[E_a(\alpha),T]_i\beta_j}{I[E_a(\propto\alpha),T]_j\beta_i}=6 \qquad \text{for } n=3 \qquad (18)$$

From the above equation, apparent activation energy for curing from the DSC curves and degradation from the thermogravimetric curves for any systems can be calculated.

Friedman Method

This is one of the differential methods used to calculate E_a, and the equation is[28]:

$$\ln\left(\frac{d\alpha}{dt}\right)=\ln(z)+n\ln(1-\alpha)-\left(\frac{E_a}{RT}\right) \qquad (19)$$

From the slope $(-E_a/R)$ of the linear plot between $\ln(d\alpha/dt)$ vs. $1/T$, the activation energy (E_a) of the system can be calculated.

RESULTS AND DISCUSSION

DSC Studies

The DSC curves recorded at $\beta = 20$°C/min for HPMI and its functionalized monomers and the DSC curves for HPMI at different heating rates (β) (10, 20, and 30°C/min) are shown in Figure 1(A,B), respectively. For clarity, the curves are shifted in the ordinate by using a common factor for each curve. The parameters such as melting temperature (T_m), enthalpy of fusion (ΔH_f), and enthalpy of curing (ΔH_c) derived from the DSC traces recorded at different β values for HPMI and its functionalized monomers are presented in Table I. The compound HPMI showed a sharp melting (T_m) at 185°C and the enthalpy of fusion (ΔH_f) was 122 J/g when the material is heated at a rate of 10°C/min. The onset of curing (T_s) was noted at around 238°C, curing attained a maximum (T_{max}) at 307°C and ended (T_E) at 346°C. The enthalpy of curing (ΔH_c) was 167 J/g and the temperature region of the curing window was 108°C. Increasing the heating rate shifts the onset (T_s) of curing from 238 to 362°C. Similarly in the case of AHPMI, MAHPMI, ALHPMI, PRHPMI and CNHPMI, increasing the heating rate shifts the curing onset temperature to higher temperatures (Table I).

Cure Kinetic Studies

Three different kinetic methods FWO,[22] VYZ,[27] and FRD[28] were used for investigating the kinetics of curing of HPMI and its functionalized monomers, AHPMI, MAHPMI, ALHPMI, PRHPMI, and CNHPMI. The plots between E_a and the reaction extent (α) of all the above mentioned monomers using FWO method are shown in Figure 2(A). The plots between E_a and the reaction extent (α) values for PRHPMI by the different

Table I. DSC Studies of HPMI and Its Functionalized Monomers at Different Heating Rates

Sample	β (°C/min)	T_m (°C)	ΔH_f (J/g)	Onset T_S (°C)	Endset T_E (°C)	$T_E - T_S$ (°C)	Maximum (°C)	ΔH_c (J/g)
HPMI	10	185	122	238	346	108	307	167
	20	186	120	244	349	148	291	183
	30	186	122	262	340	138	295	197
AHPMI	10	152	72	215	313	98	269	264
	20	153	79	226	325	99	283	263
	30	153	81	241	330	89	296	232
MAHPMI	10	154	83	184	265	81	223	175
	20	155	78	194	298	104	241	209
	30	156	79	199	298	99	257	166
ALHPMI	10	156	44	168	296	128	264	479
	20	154	45	173	312	139	257	416
	30	153	45	177	318	141	252	379
PRHPMI	10	144	29	175	338	163	270	1094
	20	146	32	178	324	146	257	1010
	30	147	32	181	330	149	265	939
CNHPMI	10	110	20	149	310	161	260	217
	20	111	25	164	321	160	251	190
	30	113	26	171	339	200	258	323

kinetic methods (FWO, VYZ, and FRD) are shown in Figure 2(B). The trend for the apparent activation energy values calculated for the curing of HPMI and functionalized monomers by the FWO and VYZ methods were the same, but the trend obtained by the FRD method differed from those obtained by the other two methods [Figure 2(B)]. This was because of the way in which E_a was calculated; that is, the VYZ and FWO methods are integral methods and FRD is a differential method. The trend in the variation of E_a for the curing of the different materials investigated is very much dependent on the nature of the functional group that is present in the monomer.

The following recommendation was developed by the Kinetics Committee of the International Confederation for Thermal Analysis and Calorimetry, the relative experimental errors in the kinetic data are larger at the lowest and highest conversions, it might be advisable to limit analysis to certain ranges. After, a reaction extent value of 0.8, vitrification is caused in thermoset matrix systems by a shift from a kinetic to a diffusion control reaction. Hill et al.[29] studied the kinetics and curing mechanism of a BMIX-diamine thermoset matrix systems. They explained that an excellent fit to the experimental data for the consumption of primary and secondary amines was obtained with the kinetic rate laws up to ~70% conversion. At higher conversions, a negative deviation from the predicted rates was found. This was attributed to vitrification, which led to an element of diffusion control in the reaction. The effect of diffusion control could be accounted for by the inclusion in the kinetic equation a term related to the T_g of the network and an E_a for segmental motion. So, in the present investigation the reaction extent values of 0.2–0.8 are only considered.

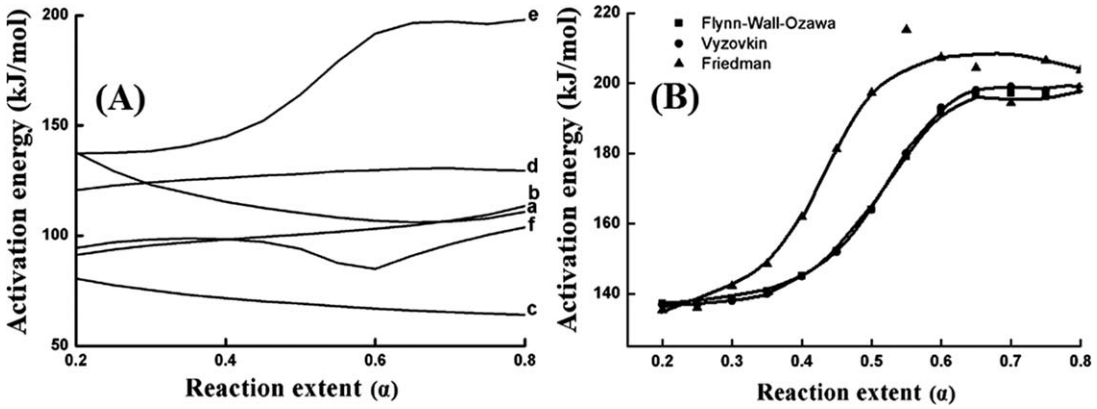

Figure 2. Comparison of apparent activation energy for curing by FWO (A) method: (a) HPMI, (b) AHPMI, (c) MAHPMI, (d) ALHPMI, (e) PRHPMI, and (f) CNHPMI. Relative reaction extent versus activation energies of curing of PRHPMI by FWO, VYZ and FRD methods (B).

In this study, E_a value calculated by the FWO method for the HPMI polymerization decreased from 138 to 111 kJ/mol when the extent of the reaction (α) increased from 0.2 to 0.8 (Figure 2). Because of the autocatalytic effect of the maleimide unit present in HPMI, initially a slight decrease in the activation energy is noted during the thermal curing of HPMI. Owing to the bifunctionality of the monomer, HPMI polymerizes to yield linear polymer chains and hence the monomer is comparatively freely available for the polymerization process. This is reflected in the E_a value and is decreased progressively up to the reaction extent at 0.7. Such a decrease in activation energy during initial cure stage has been reported by Sheng et al.[30] They studied the curing kinetics of Bisphenol E cyanate ester (BECy) resin system. They observed that the activation energy initially decreases with increase of conversion, reaching a minimum value at 30% conversion and then increases, until about 70% conversion.

From Figure 2, one can easily understand the effect of functionalization of HPMI on the polymerization of the materials. The variation of the E_a values with respect to increase in α values for the materials HPMI and MAHPMI is very similar. The monomer MAHPMI needs the least activation energy for polymerization. Acryloly and allyl (AHPMI and ALHPMI) functionalized systems behave in a similar fashion. Both PRHPMI and CNHPMI materials cure entirely in a different fashion as evidenced by the E_a value variation with respect to α value.

In the case of MAHPMI the E_a values gradually decreased (81–64 kJ/mol) with increasing extent of reaction ($\alpha = 0.2$–0.8). Regunathan Nair et al.[31] studied the copolymerization of *N*-(4-hydroxy phenyl) maleimide (HPMI) with butyl acrylate (BuA), methyl methacrylate (MMA) and styrene in dimethyl formamide (DMF) and dioxane and reported that the apparent reactivity of HPMI increased in the case of BuA and decreased in cases of both MMA and styrene. Batch and Macosko[32] found similar results for a vinyl ester resin and argued that the termination rate constant decreased with increased concentration of crosslinking species (i.e., the dimethacrylate) which raised the polymerization rate. Similar argument may be valid for this system in the present investigation.

The apparent activation energy values for AHPMI were observed to increase (91–113 kJ/mol) gradually with increasing extent of reaction ($\alpha = 0.2$–0.8) using FWO method. In the case of AHPMI during the polymerization reaction the crosslinking reaction may be taking place between acryloyl double bond and maleimide double bond. Even though the crosslinking reactions are proceeding, it is not affecting the availability of the monomer and also may be the vitrification is comparatively low. So in this case, the polymerization reactions are proceeding smoothly. Hence the activation energy increases due to increasing crosslinking and decreasing number of polymerizable groups as the reaction progresses in AHPMI. The possible polymerization of AHPMI and MAHPMI are shown in Scheme 2.

The ALHPMI shows increasing apparent activation energy value from 121 to 130 kJ/mol with increasing extent of reaction (α) from 0.2 to 0.8 (Figure 2). Xiong et al.[33] studied the copolymerization of bismaleimide containing phthalide cardo structure (BMIP) with 2,2-diallyl bisphenol A (DABPA) and they

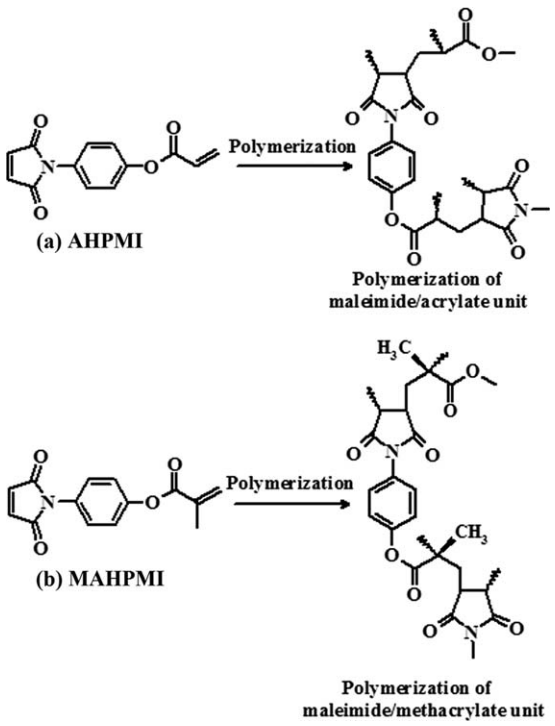

Scheme 2. The possible cure reactions of (a) AHPMI and (b) MAHPMI.

reported that the polymerization of allyl group, thermally initiated at high temperature, is also difficult because of the resulting allyl radical possesses an ability to stabilize itself by resonance.[34] Therefore, allyl polymerization shows higher apparent activation energy values. The kinetics of the curing of allyl poly(phenylene oxide) by Wang et al.[35] using the Kissinger equation[36] resulted in the E_a of allyl homopolymerization and was found to be 121 kJ/mol, a value similar to the value obtained for the polymerization of ALHPMI.

The E_a value for PRHPMI increases dramatically from 137 to 198 kJ/mol with increasing extent of reaction. Initially, the concentration of the monomer (PRHPMI) was high and hence, the polymerization reaction was easier and required low energy for the reaction. As the reaction proceeded, apart from increase in viscosity, the availability of the monomer for the polymerization is decreased. This increase in viscosity and the dearth in the polymerizable groups made the crosslinking reaction difficult. As the temperature increased linearly in the nonisothermal experiments, the chain mobility increased and the chemical reactions were reactivated. This results an increase in the activation energy for the higher reaction extent levels.[37] So at this stage, the system needs higher energy for polymerization and so the apparent activation energy gradually increased. As the extent of the polymerization is nearing completion, the higher viscosity of the medium causes vitrification and the availability of monomer and polymerizable groups is extremely low. The rate of crosslinking was limited by the mobility of the longer polymer chains and diffusion encountered a large energy barrier because of the cooperative nature of the motions. This led to higher activation energy values. So, the apparent activation energy for the polymerization was comparatively higher at the

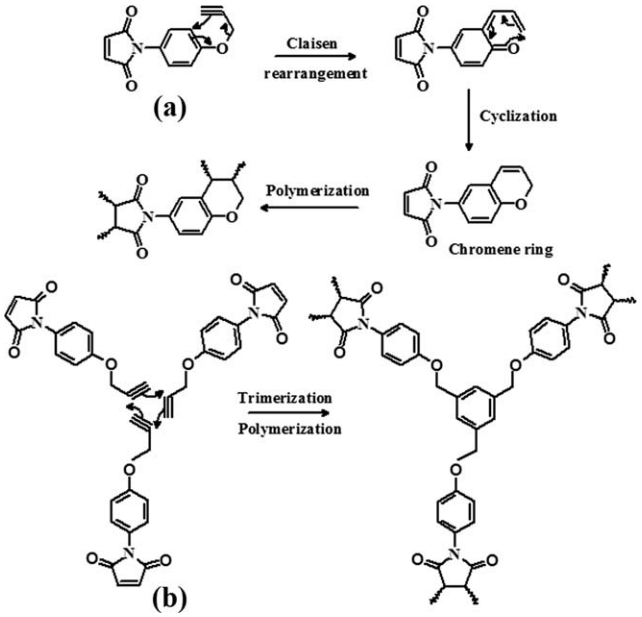

Scheme 3. The possible cure reactions of PRHPMI (a) Claisen rearrangement and (b) trimerization.

final stages of polymerization[38,39] in comparison to the initial polymerization. Liu et al.[40] reported similar results for the cure kinetics of *N*-(2-propargyloxyphenyl) maleimide, *N*-(3-propargyl-oxyphenyl) maleimide, *N*-(4-propargyloxyphenyl) maleimide and found the apparent activation energy values were in the range 150–200 kJ/mol. Because of the electron with drawing property the maleimide group, it can react with electron donating group via addition reaction. And also the acetylene compounds can copolymerize with maleimide group via Diels–Alder reaction. Further the steep increase in the E_a values after $\alpha = 0.4$ may also due to the higher energy needed for the Claisen type rearrangement in the monomer leading to the formation of chromene rings wherein the double bond present in the chromene ring (Scheme 3) system needs more energy to polymerize with similar groups and also with the double bond in the maleimide ring.

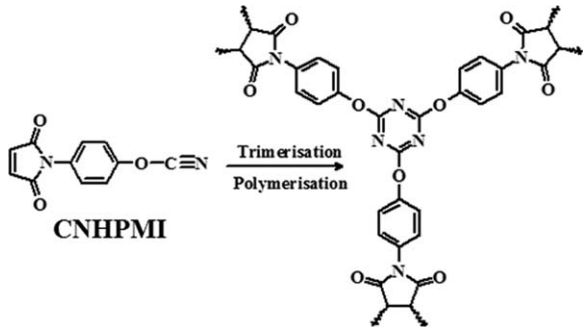

Scheme 4. The possible cure reaction of CNHPMI.

The apparent activation energy of CNHPMI increases initially from 94 to 99 kJ/mol for the reaction extent levels of 0.1–0.35 then it decreases (98–85 kJ/mol) for $\alpha = 0.4$–0.6 and then E_a value increases for further reaction extent levels. The decrease in activation energy may be due to the auto catalytic effect of the curing process and the subsequent increase of activation energy may be caused by the formation of crosslinked network (Scheme 4), which restricts diffusion of unreacted monomer. The decrease of activation energy at high conversion is still a question. At high conversion the reaction no longer follow the autocatalytic kinetic and more complex mechanism, such as diffusion control are involved in the cure process.

Swelling Studies

The results of swelling studies for PHPMI, PAHPMI, PMAHPMI, PALHPMI, PPRHPMI, and PCNHPMI are shown in Figure 3. Of all the polymers investigated the polymers PCNHPMI and PPRHPMI shows the lowest swelling ratio value (10 and 12%) and the highest swelling ratio values are noted in PHPMI (18%). Because during the polymerization reaction of CNHPMI and PRHPMI, the cyanate functionalized material is prone to trimerize and form cyanurate ring and propargyl functionalized material after Claisen type rearrangement form chromene ring, which further enters in crosslinking reactions. Because of these factors, both PCNHPMI and PPRHPMI end up with highly crosslinked networks compared to the other materials investigated. Generally, the crosslinker concentration is

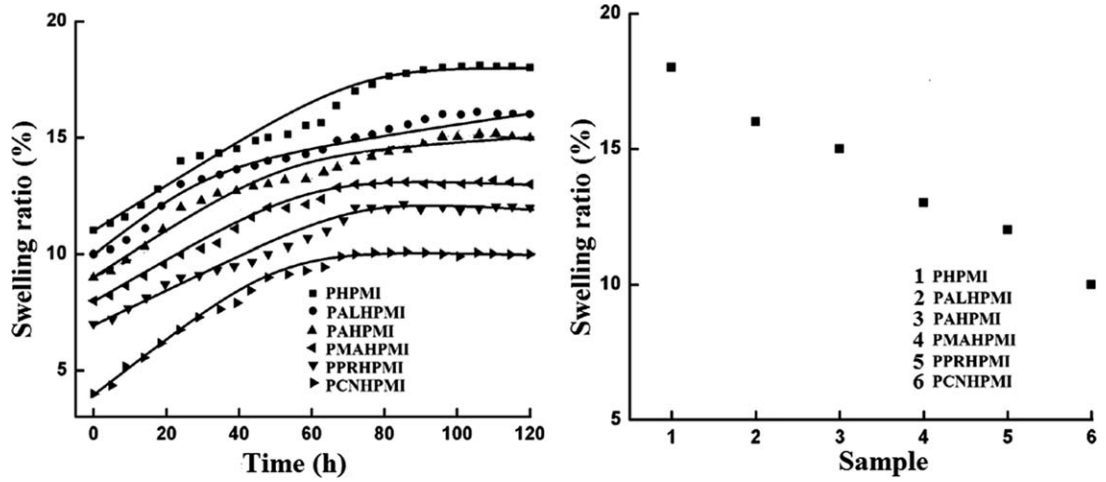

Figure 3. Comparison of swelling studies for synthesized polymers PHPMI, PAHPMI, PMAHPMI, PALHPMI, PPRHPMI, and PCNHPMI.

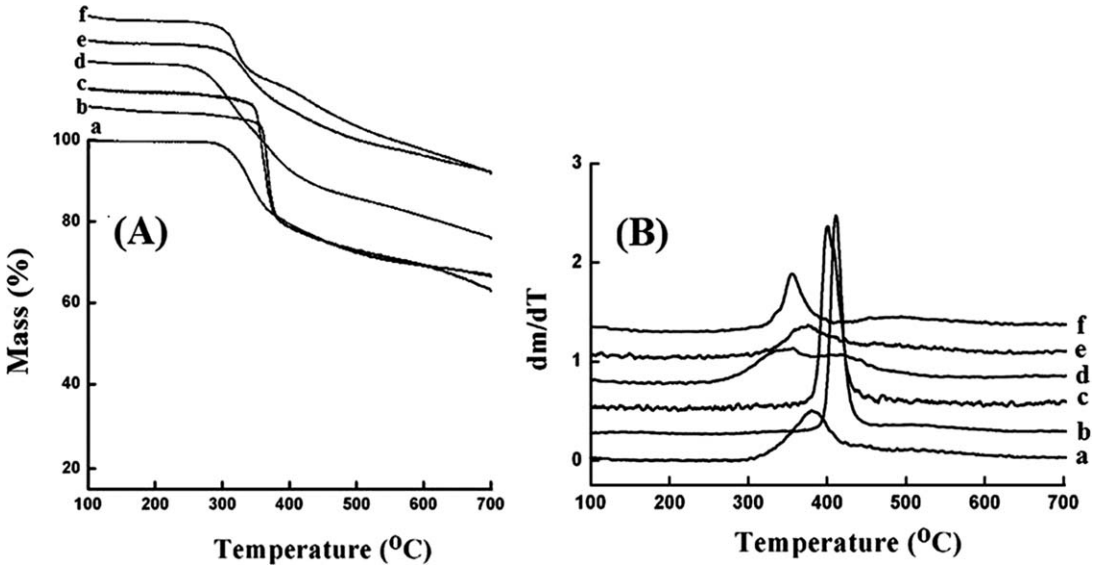

Figure 4. TGA (A) and DTG (B) traces of thermally cured HPMI and its functionalized polymers at a heating rate of 10°C/min (A): (a) PHPMI, (b) PAHPMI, (c) PMAHPMI, (d) PALHPMI, (e) PPRHPMI, and (f) PCNHPMI. For clarity, the curves are shifted in the ordinate by using a common factor for each curve.

directly related to the density of crosslinks in the polymers. At lower crosslinker concentration, the polymers may have lower crosslinking density and hence higher swelling capacity. Whereas the polymers formed with high crosslinker concentrations will possess higher crosslinking density causing a decrease in the distance between the crosslink points, there by lowering the swelling capacity.[41,42]

TG Studies

The TG and DTG curves for thermally cured HPMI and its functionalized monomers recorded at 10°C/min in nitrogen atmosphere are shown in Figure 4(A,B). The TG and DTG traces for PAHPMI recorded at multiple heating rates (10, 20, and 30°C/min) in nitrogen atmosphere are shown in Figure 5(A,B). All the thermograms are shifted to higher temperatures with increasing heating rates. The onset, maximum, endset temperatures for the degradation and the char residue obtained at 700°C for all the samples noted at multiple heating rates (10, 20, and 30°C/min) are tabulated in Table II. The detailed observations of the thermogravimetric data for the samples obtained at a heating rate of 20°C/min are discussed. The DTG curve of thermally cured HPMI shows two degradations overlapping each other indicating that the second degradation of the PHPMI starts before the completion of the first degradation [Figure 4(B)]. The initial weight loss starts at around 290°C and the second weight loss starts at 480°C. The amount of char left over at 700°C is found to be 33%. The introduction of reactive functional groups in HPMI and the polymers derived from them by thermal curing, PAHPMI, PMAHPMI, PALHPMI, PPRHPMI, and PCNHPMI, shifts the initial degradation temperature to 402, 373, 256, 325, and 341°C, respectively, a heating rate of 20°C/min. Among the different functionalizations, PAHPMI and PMAHPMI show very fast degradation as evidenced by the DTG curves [Figure 4(B)]. The polymers PHPMI, PALHPMI, PPRHPMI, and PCNHPMI show bimodal degradation pattern and the nature of degradation and volatiles evolved during these stages need further investigations since the polymerization reaction of both ALHPMI and PRHPMI is

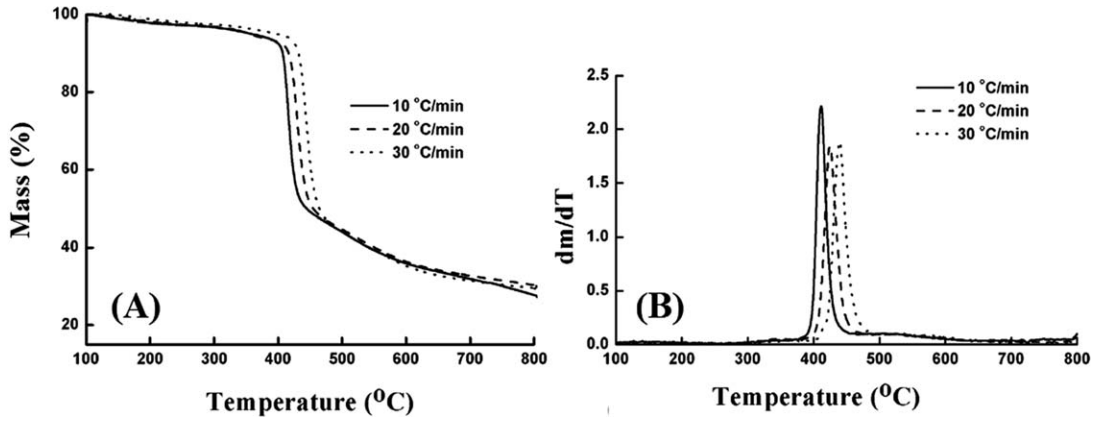

Figure 5. TG and DTG traces of thermally cured AHPMI at different heating rate.

Table II. Data Obtained from the Thermogravimetric Curves of Thermally Cured HPMI and Its Functionalized Monomers at Different Heating Rates

Sample	Heating rate (°C/min)	Onset T_S (°C)	Maximum (°C)	Endset T_E (°C)	Char value at 700°C (%)
PHPMI	10	279	380	671	31
	20	290	400	687	33
	30	313	421	693	32
PAHPMI	10	376	411	622	30
	20	402	425	635	32
	30	414	439	647	33
PMAHPMI	10	361	401	574	24
	20	373	427	592	26
	30	380	429	612	26
PALHPMI	10	248	356	595	32
	20	256	372	608	33
	30	303	384	619	33
PPRHPMI	10	290	376	623	47
	20	325	391	657	49
	30	334	397	668	48
PCNHPMI	10	320	356	668	40
	20	341	368	683	40
	30	349	381	696	41

complicated by the Claisen rearrangement reaction. In the polymerization of CNHPMI, the trimerization of the cyanate entities to triazene rings and the participation of the maleimide double bond in the cyclization reactions with cyanates lead to complex structures.

Degradation Kinetics

The apparent activation energy for the degradation of PHPMI and its functionalized polymers (PAHPMI, PMAHPMI, PALHPMI, PPRHPMI, and PCNHPMI) were determined by three different model-free kinetic (FWO, VYZ, and FRD) methods. The plots between the apparent activation energy (E_a) and reaction extent (α) values for the all the materials investigated by VYZ method are shown in Figure 6(A). The plots between the apparent activation energy and the reaction extent values of PMAHPMI by all the methods are shown in Figure 6(B). Here also the trends noted in the variation of apparent activation energy for the degradation of cured samples obtained by the three kinetic methods are same like curing kinetics.

Jankovic et al.[43] studied the kinetics of the nonisothermal dehydration of equilibrium swollen poly(acrylic acid) hydrogels with thermogravimetric analysis by five different isoconversional methods [FRD, FWO, KAS, Tang (T), and VYZ]. The change in E_a with respect to the reaction extent for the methods FWO, KAS, T, and VYZ led to close values of E_a, but these values differed substantially from the values of E_a obtained with the isoconversional method suggested by FRD.

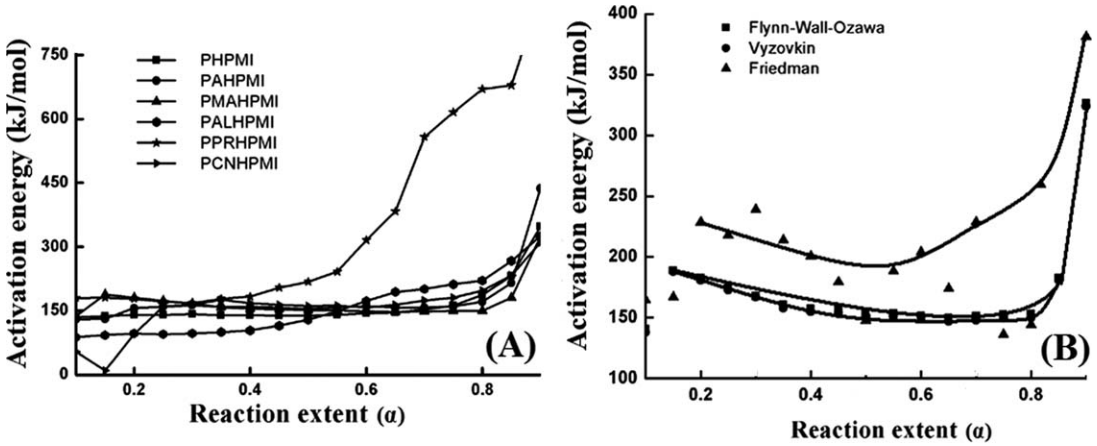

Figure 6. Comparison of apparent activation energy for degradation by VYZ (A) method: (a) PHPMI, (b) PAHPMI, (c) PMAHPMI, (d) PALHPMI, (e) PPRHPMI, and (f) PCNHPMI. Relative reaction extent versus activation energies of degradation of PMAHPMI by FWO, VYZ, and FRD methods (B).

The apparent activation energy for thermal degradation obtained using VYZ method for thermally cured HPMI and its functionalized polymers are considered for the discussion. The apparent activation energy for the degradation of PHPMI varies from 98 to 348 kJ/mol. A slight decrease in apparent activation energy is noted for the initial reaction extent levels (0.25–0.5), and increases constantly up to the reaction extent level $\alpha = 0.75$, then sudden increase is noted for further reaction extent levels. Similar variation in E_a values for different α values has been reported by Surender et al.[44] in the thermal degradation studies on polymer derived from the thermal polymerization of Bisphenol-A based bismaleimide (BMIX), The apparent activation energy for the degradation of poly-BMIX varies from 187 to 258 kJ/mol. A slight decrease in apparent activation energy is noted for the initial reaction extent levels (0.1–0.4), and increases constantly up to the reaction extent level $\alpha = 0.65$, then sudden increase is noted for further reaction extent levels.

Except PAHPMI, the degradation kinetics of all other materials investigated PMAHPMI, PALHPMI, PPRHPMI, and PCNHPMI, show higher apparent activation energy values when compared to the values for PHPMI. In the case of PAHPMI, the apparent activation energy ($\alpha = 0.2$–0.8) for the thermal degradation is low compared to PHPMI. During the polymerization of AHPMI, the possibility of the copolymerization of the double bond present in the acrylate part with the double bond in the maleimide part exists and it will form a crosslinked network structure. The bond breaking through the β-scission route is possible in PAHPMI and hence needs lesser energy for the degradation

Kandare et al.[45] studied the thermal stability and degradation kinetics of poly(methyl methacrylate) (PMMA)/layered copper hydroxy methacrylate composites. They reported that the E_a value for the pure commercial PMMA, as received, decreased from 160 to 110 kJ mol^{-1} between $\alpha = 0.05$ and 0.55. The E_a value then increased in a parabolic fashion to a value of 180 kJ mol^{-1} at $\alpha = 0.9$. Laachachi et al.[46] reported similar results for the thermal degradation of PMMA in air. Similarly, in our study, the apparent activation energy value for the PMAHPMI decreased from 188 to 147 kJ mol^{-1} between $\alpha = 0.15$ and 0.65 then the E_a value increased to a value of 324 kJ mol^{-1} at $\alpha = 0.9$. This may be attributed to the structural characteristics of PMAHPMI.

In the case of PALHPMI, initially the apparent activation energy shows lower value at the reaction extent of 0.1–0.5 (88–129 kJ/mol) compared to pure PHPMI (98–139 kJ/mol) but after that reaction extent levels ($\alpha = 0.55$–0.85), the E_a value is high (149–267 kJ/mol) compared PHPMI (141–232 kJ/mol). This may be due to the complex structures produced during the thermal polymerization of ALHPMI wherein the double bonds of the allyl group, allyl group generated due to Claisen rearrangement and the maleimide group are involved.

Of all the polymers investigated, polymer PPRHPMI showed the highest E_a values and they range from 183 to 671 kJ/mol. Initially, the E_a values show a slight decrease (from 183 to 178 kJ/mol) with increasing reaction extend values ($\alpha = 0.1$–0.35). After that the E_a values gradually increase up to $\alpha = 0.65$ and then a steep increase in the apparent activation energy values is seen. It was probably due to during the polymerization reaction phenyl propargyl ether could undergo Claisen type sigmatropic rearrangement to form a chromene ring by an intramolecular ring formation reaction resulting from the thermal excitation. The double bond present in the chromene ring also undergoes polymerization. Hence during the thermal degradation of PPRHPMI, the possibility for aromatization leading to char is inevitable. Owing to char formation after a particular stage of degradation, further degradation requires high energies. This is reflected in the char value noted for PPRHPMI. Reghunathan Nair et al.[47] investigated the thermal characteristics of propargyl ether phenolic resins. They associated the second stage of thermal degradation to the carbonization process.

The apparent activation energy values for the degradation of PCNHPMI increased from 54 to 310 kJ/mol gradually with increasing extent of reaction ($\alpha = 0.2$–0.8). Because during the curing process of CNHPMI, apart from the trimerization of the cyanate groups, the bismaleimides double bond entering in the cyclization reaction with the cyanate groups is highly probable. Hence PCNHPMI needs higher energies for the thermal degradation compared to PHPMI.

CONCLUSIONS

The functionalization of the maleimide monomer with different cross linkable groups (acryloyl, methacryloyl, allyl, propargyl, and cyanate) was carried out and the structures were confirmed by FTIR and NMR studies. The DSC studies showed the introduction of polymerizable functional groups in HPMI leads to decrease in the curing temperature. The acryloyl and methacryloyl functionalizations considerably increase the degradation temperature of the polymers whereas functionalizations using cyanate and propargyl groups boost the char formation of the thermoset. The curing kinetics of HPMI and its functionalized monomers and the degradation kinetics of poly-HPMI and its functionalized polymers were studied using three model-free kinetic methods such as FWO, Vyazovkin, and Freidman. The apparent activation energy for the curing of HPMI decreased, as the extent of polymerization increased. Among the various functionalization the curing kinetics of AHPMI, MAHPMI, and CNHPMI shows the lowest activation energy value compared to HPMI, whereas ALHPMI and PRHPMI shows highest E_a value. The apparent activation energy values for the thermal degradation of the functionalized polymers are high compared to PHPMI. A constant increase in the apparent activation energy trend is noted for the degradation all the materials investigated. Because of the formation of crosslinked network structure in the investigated functionalized polymers, higher activation energy is needed for the degradation.

ACKNOWLEDGMENTS

The authors thank the Board of Research in Nuclear Science (BRNS), Department of Atomic Energy (DAE), Government of India, BARC, Mumbai 400 085 for financially supporting this work under the Grant 2010/35/5/BRNS/1279 dated 11-08-2010. They also thank Lalit Varshney and K. S. S. Sharma of BARC for their constant encouragement and support. Sincere thanks to the

Management and the Principal of Kamaraj College of Engineering and Technology, S.P.G.C. Nagar, K. Vellakulam Post 625701, India for providing all the facilities to do this work.

REFERENCES

1. Hiran, B. L.; Paliwal, S. N.; Choudhary, J. E. *J. Chem.* **2007**, *4*, 265.
2. Mittal, K. L.; Polyimides: Synthesis Characterisation, and Application; Plenum Press: New York, **1894**, p 1 and 2.
3. Cuppon, R. C. P. *Polymer* **1965**, *6*, 419.
4. Hiran, B. L.; Boriwal, R.; Bapana, S.; Paliwal, S. N. *J. Univ. Chem. Technol. Metallurgy.* **2010**, *45*, 127.
5. Ali, E. A.; Mokhtar, S. M.; Elsabee, M. Z. *Polym.-Plast. Technol.* **2010**, *49*, 953.
6. Elkholy, S. S. *Polym.-Plast. Technol.* **2010**, *47*, 299.
7. Bilici, A.; Doğan, F.; Yıldırım, M.; Kaya, İ. *React. Funct. Polym.* **2011**, *71*, 675.
8. Barrales-Rienda, J. M.; Mazón-Arechederra, J. M. *Polymer* **1987**, *28*, 788.
9. Sugiura, M.; Murase, A.; Mitsuoka, T. *Polym. Degrad. Stab.* **2001**, *72*, 393.
10. Coşkun, M.; Ilter, Z. *J. Polym. Sci. Part A. Polym. Chem.* **2002**, *40*, 1184.
11. Ninomiya, A.; Daisuke, H. K.; Hiroharu, A. *Sci. Technol. Adv. Mater.* **2006**, *7*, 162.
12. Dirlikov, S. K. *High. Perform. Polym.* **1990**, *2*, 67.
13. Saha, B.; Ghoshal, A. K. *Thermochim. Acta.* **2006**, *451*, 27.
14. Vyazovkin, S.; Wight, C. A. *Thermochim. Acta.* **1999**, *340/341*, 53.
15. Vyazovkin, S. *Thermochim. Acta.* **1999**, *355*, 155.
16. Vyazovkin, S.; Wight, C. A. *Chem. Mater.* **1999**, *11*, 3386.
17. Vyazovkin, S.; Dollimore, D. *J. Chem. Inf. Model.* **1999**, *36*, 42.
18. Vyazovkin, S. *Int. J. Chem. Kinet.* **1996**, *28*, 95.
19. Pitchaimari, G.; Vijayakumar, C. T. *J. Therm. Anal. Calorim.*, DOI 10.1007/s10973-013-3174-4.
20. Muralimohan, Y.: Sudhakar, K.: Kesavamurthy, P. S.; Mohanraju, K. *Int. J. Polym. Mater.* **2006**, *55*, 513.
21. Vinayagamoorthi, S.; Vijayakumar, C. T.; Alam, S.; Nanjundan, S. *Eur. Polym. J.* **2009**, *45*, 1217.
22. Yei, D. R.; Fu, H. K.; Chen, W. Y.; Chang, F. C. *J. Polym. Sci. Polym. Phys.* **2006**, *44*, 347.
23. Budrugeac, P.; Segal, E. *Int. J. Chem. Kinet.* **2001**, *33*, 564.
24. Doyle, C. D. *J. Appl. Polym. Sci.* **1962**, *6*, 639.
25. Coats, A. W.; Redfern, J. P. *Nature* **1964**, *201*, 68.
26. Gorbachev, V. M. *J. Therm. Anal. Calorim.* **1975**, *8*, 349.
27. Vyazovkin, S.; Burnhamb, A. K.; Criadoc, J. M.; Perez-Maquedac, L. A.; Popescud, C.; Sbirrazzuolie, N. *Thermochim. Acta.* **2011**, *520*, 1.
28. Tarase, M. V.; Zade, A. B.; Gurnule, W. B. *J. Appl. Polym. Sci.* **2010**, *116*, 619.
29. Hopewell, J. L.; Georgeb, G. A.; Hilla, D. J. T. *Polymer* **2000**, *41*, 8221.
30. Sheng, X.; Aknic, M.; Kessler, M. R. *J. Therm. Anal. Calorim.* **2008**, *93*, 77.
31. Reghunadhan Nair, C. P.; Mathew, D.; Ninan, K. N. *Eur. Polym. J.* **1999**, *35*, 1829.
32. Batch, G. L.; Macosko, C. W. *J. Appl. Polym. Sci.* **1992**, *44*, 1711.
33. Xionga, X.; Chena, P.; Zhanga, J.; Wang, Q. *Thermochim. Acta.* **2011**, *514*, 44.
34. Matsumoto, A. *Prog. Polym. Sci.* **2001**, *26*,189.
35. Wang, L. H.; Xu, Q. Y.; Chen, D. H. *J. Appl. Polym. Sci.* **2006**, *102*, 4111.
36. Kissinger, H. E. *Anal. Chem.* **1957**, *29*, 1702.
37. Guigo, N.; Mija, A.; Vincent, L.; Sbirrazzuoli, N. *Phys. Chem. Chem. Phys.* **2007**, *9*, 5359.
38. Gao, W.; Cao, J.; Li, *J. Iran. Polym. J.* **2010**, *19*, 959.
39. Gao, W.; Cao, J.; Li, *J. Iran. Polym. J.* **2010**, *19*, 255.
40. Liu, F.; Liu, J. T.; Zhao, T. *J. Appl. Polym. Sci.* **2010**, *115*, 3103.
41. Stezenberger, H. D. *Adv. Polym. Sci.* **1994**, *117*, 165.
42. Hiremath, J. N.; Vishalakshi, B. *Der. Pharm. Chem.* **2012**, *4*, 946.
43. Jankovic, B.; Adnadevic, B. *J. Thermochim. Acta.* **2007**, *452*, 106.
44. Surender, R.; Mahendran, A.; Thamaraichelvan, A.; Alam, S.; Vijayakumar, C. T. *Thermochem. Acta* **2013**, *562*, 11.
45. Kandare, E.; Deng, H.; Wang, D.; Hossenlopp, J. M. *J. Polym. Adv. Technol.* **2006**, *17*, 4.
46. Laachachi, A.; Cochez, M.; Ferriol, M.; Leroy, E.; Lopez Cuesta, J. M.; Oget, N. *Polym. Degrad. Stab.* **2004**, *85*, 641.
47. Regunathan Nair, C. P.; Bindu, R. L.; Krishnan, K.; Ninan, K. L. *Polym. Degrad. Stabil.* **1999**, *35*, 235.